Research Article

Chemical Review and Letters
journal homepage: www.chemrevlett.com
ISSN (online): 2645-4947(print) 2676-7279

Preparation and application of Loess-based adsorbent for the removal of lead ions from aqueous solution

Tehmina Bano[1, *]

[1]*Master's in Chemical Engineering and Technology, Chang'an University Shaanxi, Xi'an China*

ARTICLE INFO

Article history:
Received 5 November 2024
Received in revised form 28 November 2024
Accepted 29 November 2024
Available online 15 December 2024

Keywords:
Polymerization
Loess
Adsorption
Lead Ions
Wastewater

ABSTRACT

In this study a loess clay-based co-polymer, KHLC/PAA, was produced to support the functional monomer acrylic acid in an in situ polymerization process using N-N methylene bisacrylamide as a cross-linking agent. It was characterized by Scanning Electron Microscopy, Fourier Transformation Infrared spectroscopy, X-ray diffractometry, X-ray fluorescence spectroscopy, and thermal gravimetric analysis, followed by the examination of its adsorption capability for removing lead ions (Pb2+) from aqueous solution at room temperature in 60 minutes, which appeared to be 159.1 mg/g. The thermodynamic data showed that the adsorption process was practicable, spontaneous, and endothermic, and the experimental results suited the pseudo-second-order kinetic model and the Langmuir adsorption isotherm well. Pb(II) adsorption on KHLC/PAA was fitted to the Langmuir monolayer adsorption model, proving that its isothermal equation is better for test findings. The thermodynamic measurements showed spontaneous, practical, endothermic Pb2+ adsorption on KHLC/PAA. The computed maximum adsorption capacity (qm) of Pb2+ ions on KHLC/PAA was 159.1mg/g at 25°C and pH 5, with 92.2% removal efficiency. KHLC/PAA-Pb FTIR data analysis indicated surface complexation and ion exchange as adsorption processes. Consequently, KHLC/PAA is a potentially beneficial material for wastewater treatment as it is an inexpensive, environment-friendly adsorbent.

1. Introduction

The most significant and necessary element on earth for the survival of life is water. It is believed that there are 1388 million billion cubic meters of water on Earth. One-third of the world's population uses groundwater for drinking, whereas, one-sixth (nearly 2 billion), live in developing nations without access to clean drinking water[1], 2.6 billion people lack basic sanitation facilities, and the current rarity and contamination of drinking water pose a threat to global water supplies. Water pollution is the most common form of environmental contamination, which has long been a serious and deadly issue for humans. The discharge of wastewater resulting from industrial production has grown increasingly problematic in today's fast-developing industrial civilization, leading to varying degrees of contamination in rivers and lakes [2, 3]. Among these is the threat to human health and survival due to human-caused heavy metal pollution in water. Heavy metal ions in wastewater can enter the human body through biological circulation, hence threatening human health. However, the depletion of Earth's water resources and the increasing demand for clean water are compelling us to reconsider the risks posed by these pollutants and modernize wastewater treatment [4-6]. Pb^{2+} is the most prevalent hazardous metal ion in daily life, which can have

* Corresponding author; e-mail: tehminabano87@gmail.com
https://doi.org/10.22034/crl.2024.487321.1468

permanent negative effects on health in both children and adults[7]. It is widely used in the industrial sector including chemical, electrical, electronic and leather industries; along with its widespread use in jewelry, arts and crafts in developing countries[8]. Pb^{2+} poisoning among children has been common since 2009. In August of the mentioned year, wastewater discharged from a nearby smelter in Fengxiang City, Shaanxi Province, China, poisoned 851 local children. More than 170 of the children were sent to the hospital for emergency treatment, which caused the violent protests among the populace and drew attention from the government. Then, in 2011, trash from a battery factory in Huaining City, Anhui Province, resulted in elevated Pb2+ levels in the blood of 228 local children, demonstrating the potential dangers associated with heavy metal ions. As a result, wastewater treatment for heavy metal ions is about to happen [9].

Currently, various methods for the treatment of heavy metal contamination in water are being utilized including chemical precipitation, biological treatment, electrolysis, ion exchange, membrane separation, and adsorption. But these methods had few drawbacks including least selectivity for heavy metals, non-variety of functional groups, low treatment efficiencies for heavy metals, formation of toxic sludge and high operational costs[10].Up to now, the adsorption method is considered to be the most widely used method in water pollution treatment technology with its unique advantages, which are not only high efficiency, high selectivity, re-usability, and less toxicity but its simple operation, and the fact that it can remove a variety of different types of pollutants such as heavy metal ions and dyes[11]. The most important aspect in using adsorption technology to treat wastewater is the Preparation of an environmentally friendly, low-cost, and highly effective adsorbent with excellent affinity for pollutants by using a particular and suitable adsorbent. Some of the reported adsorbents used previously include activated carbon[12], zeolite[13], clay[14], and sludge soil[15]. The Preparation of adsorbent with low cost and easy availability requires a wide spread and inexpensive natural material and Chinese loess could be a best option in this regard. As being rich in composition and cheap natural material, loess can be used to remove a variety of heavy metals from aqueous solution[16]. For example, Tang et al. experimented that the calcinated Chinese loess can remove Zn^{2+} ions with the adsorption capacity of 113.6mg/g[17]. Xing et al. have found that Pb^{2+} ions can be efficiently removed by using red loess[18]. R.M Wang et al. prepared and utilized loess based adsorbent with Acrylic acid for Pb^{2+} ions removal in wastewater and they achieved removal efficiency of 99%[19]. In particular, nanocomposite and biohydrogel fields were found to be very promising for environmental and analytical applications. Hydrogel-Fe_3O_4 magnetic nanocomposites were used to remove organic dyes from wastewater and nanocomposite PU filtration as multifunctional filters used in the municipal wastewater treatment process to eliminate organic pollutants [19, 20]. In the same way, biohydrogels containing soy protein, tragacanth, mesoporous silica nanoparticles, and lycopene were used selectively to remove nitrites from sediment of the Lake Urmia [21]. Substituted sorbents Zein/EDTA/chlorophyll/nano-clay biocomposite sorbents showed excellent performance again indicating the potential of green materials for pollutant removals in industrial wastewaters [22]. Fibers of poly N-phenyl pyrrole, poly (N-methyl pyrrole-pyrrole) nanoscale applied in analytical chemistry enhanced the HS micro extraction of organic volatiles in yogurt matrix [23, 24]. The following green extraction methods; β-cyclodextrin, and ultrasound were used to extract the bioactive compounds from pomegranate peel [25]. Moreover, a Fe_3O_4/SiO_2/polypyrrole nanocomposite was prepared to desalinate edible sea salts to provide an example of this class of nanocomposites for use in the food industry or environmental conservation [26]. Altogether, the results discussed in these studies exhibit the blow of use nanotechnology and biocomposite materials for solving the world environmental and analytical problems. All these references establish that loess can be used as potential low cost adsorbent in the removal of Pb2+ ions from wastewater. This work involves the synthesis, by in-situ polymerization, of a surface grafted functional loess clay co-polymer acrylophenone (AP) / Acrylic Acid (AA) (KHLC/PAA) and investigation of adsorption of Pb2+ ions in aqueous solution. In Preparation, to reduce the cost of the composite material, a higher proportion of clay was produced accompanied by a lesser proportion of polymer and therefore the cost of producing polymer adsorbent was reduced. In endeavor to evaluate the effectiveness of KHLC/PAA on the removal of Pb^{2+} ions from aqueous solution some factors influencing the adsorption process included temperature, pH value, dosage, contact time and initial concentration of adsorbed solution were studied.

2. Experiment

2.1. Materials and Reagents

The main raw material loess (called Huangtu) was collected for free near the national highway of Xi'an Shaanxi (China). AA and N-N Methylene Bisacrylamide (MBA) are commercially available and were obtained from Tianjin Comeo Chemical Reagent company, other

chemicals including KH570 solution, ethanol, potassium persulfate, ammonia solution, acetic acid and sodium hydroxide are analytical reagents and commercially available. Distilled water was utilized throughout the experimental work.

2.2. Preparation of Adsorbent

First, LC is pre-treated with hydrochloric acid (HCl). The dried LC was ground and sieved at 100 mesh. 10.00 g of the grounded LC was added to 150 ml HCl solution (4 $mol.L^{-1}$) at 80℃ and was stirred for complete 2 hours. The solution was then allowed to cool to room temperature. The pre-treated LC was filtered, and it was then washed with distilled water until the eluents were neutral. The acidified LC (HLC) was dried at 60 ℃ for 5 h, yielding 76.5% of the required product. Secondly, the HLC is further modified by silane coupling agents KH-570. A three-necked flask was taken in which, 5.00g HLC, 10 ml H_2O and 30 ml ethanol (EtOH) were mixed and kept on stirring for 1 hour. The pH value was adjusted in between 3.0–and 4.0 after one hour by adding few drops of acetic acid (HOAc) solution. Along with that, at this step KH-570/KH-792 (1.00 g or 1ml), were added to the mixture and it was further stirred for 30 min at room temperature. Afterward, the pH value of the mixture was adjusted to 9–10 with the ammonia solution ($NH_3 \cdot H_2O$), and after that the solution is heated at 80℃ continuously with stirring for 3 hours. The product is filtered and washed with EtOH three times to remove the unreacted KH-570/KH-792. After that, the product was vacuum dried at 50℃ for 8 hours, and the final silane coupling agent modified loess (KH-LC) is obtained with a yield of 82.3% of.

2.3. Characterization of Adsorbent

The obtained loess-based grafting co-polymer KHLC/PAA was characterized by using X-ray diffraction, X-ray fluorescence techniques, and elemental analysis FTIR. XRD patterns were recorded on an XRD-6100 diffractometer using graphite monochromatic copper radiation, at 40kV, 30mA over the 2θ range from 5 to 80°, while the XRF data was collected through XRF1800-ASF(E) spectrometer. FTIR spectra were recorded between 4000 and 500 cm^{-1} by using the potassium bromide (KBr) method and registered on the IRTracer 100 spectrophotometer using KBr pallets. The pore structure and surface morphology of the adsorbents were observed by SEM images recorded on a GeminiSEM360 microscope, and the surface area and pore size of the material were determined by using the BET analysis through N_2 adsorption-desorption isotherms and pore distribution diagram.

2.4. Characteristics of Used Material

This investigation relied on natural clay mineral loess. It followed the national route from Xi'an, Shaanxi. Free Huangpu loess was recovered following processing and modification. For consistency, loess was crushed and sieved to 100 mesh during pre-treatment. Hydrochloric acid from Tianjin Comeo Chemical Reagent changed the loess. KH-570 and KH-792, available from the same source, changed the loess after acid treatment. In situ polymerization of AA and N-N methylene bisacrylamide (MBA) produced the surface-grafted functional loess-based co-polymer (KHLC/PAA). These chemicals' purity surpassed 98%, ensuring experiment effectiveness. We utilized unpurified sodium hydroxide, acetic acid, potassium persulfate, ammonia, and analytical-grade ethanol. Distilled water was used throughout the experiment to avoid contaminants. The KHLC/PAA adsorbent was characterized using advanced methods. XRD was used to investigate the loess's crystalline structure before and after alteration. The changed loess' chemical composition was evaluated by an XRF1800-ASF(E) spectrometer. The functional groups of the improved adsorbent were examined using FTIR. A GeminiSEM360 microscope examined the adsorbent's surface morphology and pore structure, which affect adsorption capacity. BET (Brunauer-Emmett-Teller) study utilising nitrogen adsorption-desorption isotherms revealed the adsorbent's surface area and pore size distribution.

2.5. Adsorption Experiments

Loess was pretreated with hydrochloric acid in many steps to make the adsorbent. Heat the mixture at 80°C for two hours after adding 150 ml of 4 mol/L HCl. After filtration, it was washed with distilled water and dried at 60°C for five hours. Loess weighed 10 grammes. Pre-treated loess was modified using silane coupling agents KH-570 and KH-792. This step included mixing 5 g HLC, 30 ml ethanol, and 10 ml water in a three-necked container. The mixture was stirred for an hour at room temperature before adding silane coupling agents. After ammonia lowered pH to 9–10, KHLC was vacuum-dried. This combination was cooked at 80°C for 3 hours. KHLC/PAA was tested for Pb2+ ion adsorption from aqueous solutions. Adsorption tests consisted of starting Pb2+ concentrations (20 mg/L to 300 mg/L), adsorbent doses (0.02 g to 0.2 g), contact periods (30 minutes to 24 hours), temperature (10°C to 50°C), and pH (2 to 9). The experiments were done in a 150-rpm shaker at a constant temperature. The residual Pb2+ was measured using the Atomic Absorption

Spectrophotometer. The removal efficiency was calculated using the equation:

$$\text{Removal Efficiency (\%)} = \frac{C_o - C_e}{C_e} \times 100 \quad 1$$

$$\text{Adsorption Efficiency} = \frac{C_o - C_e}{m} \times V \quad 2$$

where Co is the initial concentration and Ce is the equilibrium concentration of Pb2+ ions. Adsorption efficiency was calculated using the following equation:

Adsorption Efficiency=(Co−Ce)m×V

Adsorption Efficiency=m×V(Co−Ce)

where mm is the mass of the adsorbent and VV is the volume of the solution.

2.6. Desorption and Re-usability

The desorption of Pb^{2+} from KHLC/PAA was done by dissolving the adsorbent in 50mL of HCl ($0.1 mol.L^{-1}$) solution at a fixed time interval of 60 minutes and the re-usability of KHLC/PAA was evaluated by reusing it in five simultaneous adsorption cycles of Pb^{2+} adsorbed in KHLC/PAA at 25°C with the constant experimental conditions (initial concentration of each contaminant= 50mg/L, 0.1 g of adsorbent, contact time= 1h and pH=5), and the residual concentration of Pb^{2+} was calculated on AAS. Afterwards, the used adsorbent was washed several times with deionized water and ethanol-containing solution and the treated adsorbent was dried out at 60°C for 18-20 hours (or overnight) in a laboratory oven. This adsorbent was used repeatedly for five cycles.

2.7. Scheme of Work

KHLC/PAA was meticulously tested for Pb^{2+} ion adsorption from aqueous solutions. Loess was collected, processed, and treated using acrylic acid and silane coupling agents to create the functionalized adsorbent. The adsorbent's characteristics and applicability were validated by XRD, XRF, FTIR, SEM, and BET. Pb2+ concentration, adsorbent dosage, contact time, temperature, and pH were then tested by adsorption experiments. The best Pb2+ removal settings were found by examining experimental data. Regenerating KHLC/PAA with 0.1 mol/L HCl after five adsorption-desorption cycles assessed its effectiveness and reusability. Finally, the experiment measured adsorption and removal efficiency. These findings assessed KHLC/PAA's water treatment adsorption. This extensive study showed the material's ability to remove heavy metals from polluted water, enabling inexpensive, ecologically acceptable wastewater treatment systems.

3. Results and Discussion

3.1. Preparation of Adsorbent

It was found that the successful synthesis of loess-based adsorbent by grafting co-polymerization consisted of simple addition of monomers after pre-treatment of loess with HCl and KH-570.The adsorbent was prepared using acrylic acid (AA) as a monomer for the Preparation of KHLC/PAA. Hence, AA and AM were selected as the basic and suitable monomers in this work because it is a vinyl monomer and is environment friendly as it creates very less pollution. Due to the carboxylic group (–COOH) present in AA, the pH of its polymer caused an effect on the degree of ionization, which further affected the rate of polymerization. The process for Preparation of KHLC/PAA is shown in following Figure 1.

We explored that the co-polymer can be successfully grafted on the loess particle KH-LC, and the results are shown in Table 1. However, the yield (%) is decreased when another monomer i.e.; Acryl amide (AM) was used as a single monomer or in co-monomer form with AA. AM has previously been used with AA for the synthesis of a variety of useful co-polymers[20]. It was also observed that the ratio of LC to monomers and other constituents is also an important factor for Preparation and good yield (%) of the product and the ratio of LC to monomers should be more than 10:1.

Table 1. The recipes for preparing loess-based grafting co-polymer and yields (Conditions; grafting co-polymerization at 80°C for 30 min

Product	KH-LC	AA	AM	MBA	Yield (%)
	(g)	(g)	(g)	(g)	
KHLC/PAA(a)	12.5	1	0	1.54	95
KHLC/PAA(b)	6.25	1.5	0	1	87.2
KHLC/PAM	12.5	0	1.5	1.54	79
KHLC/PAA-AM(a)	12.5	1	1.5	1.54	89.4
KHLC/PAA-AM(b)	6.5	1.5	1	1	85.7

3.2. Characterization of the adsorbent

3.2.1 FTIR analysis of KHLC/PAA

The FT-IR spectra of the adsorbents (KHLC/PAs) and materials (LC, HLC, and KHLC) is shown in Figure 2.13(a,b). The LC spectra show a broad absorption peak at about 3450 cm^{-1} and a very sharp peak at 797 cm^{-1},

representing the -OH group and quartz (SiO_2), respectively. The characteristic peaks at 3626 cm^{-1} and 3450 cm^{-1} can be attributed to the stretching vibration of surface hydroxyl groups (–OH). The peaks at 3628, 1037, 694,538, and 470 cm^{-1} are assigned to the Si-O-Si stretching. In KH-LC, the characteristic absorption peak of methylene in KH-570 was near 2950 cm^{-1}, and the peak at 1716 cm^{-1} points towards

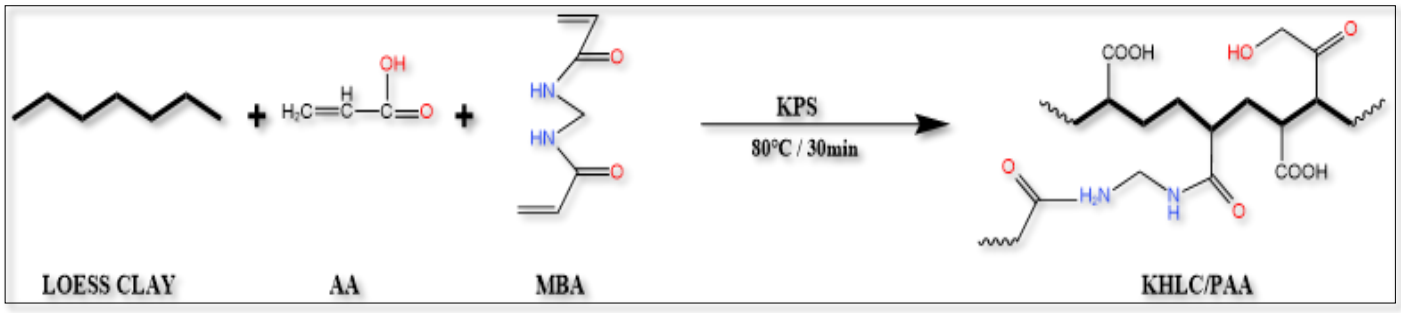

Fig. 1. Formation of KHLC/PAA

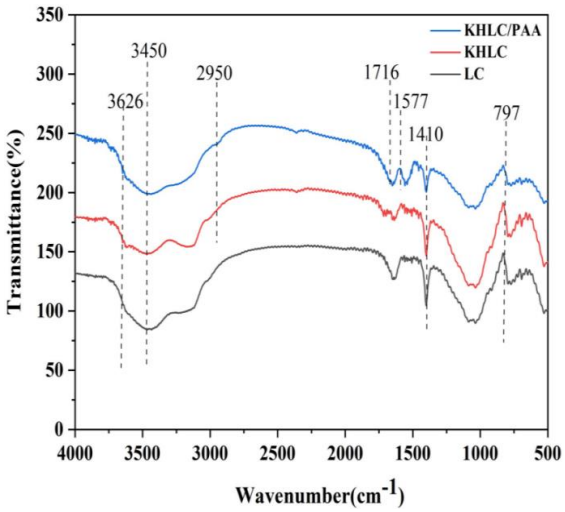

Fig. 2. The IR spectra of LC, KHLC and KHLC/PAA

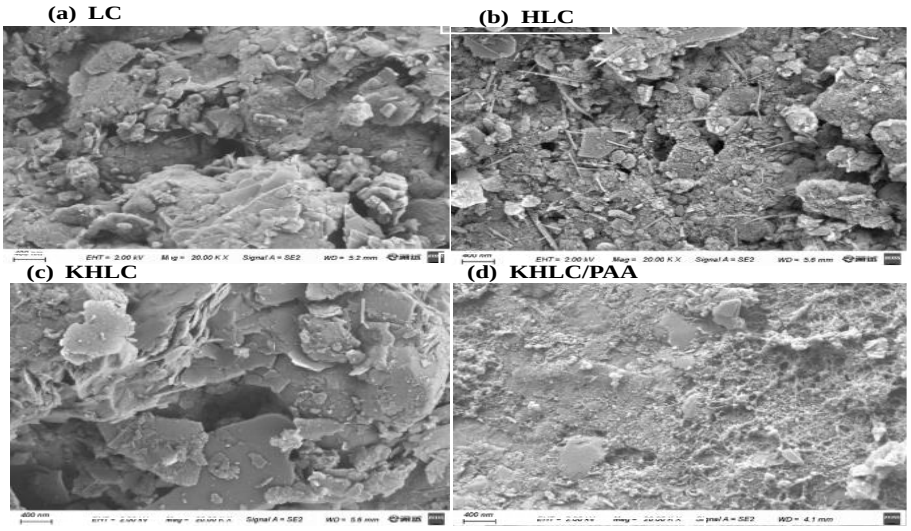

Fig. 3 . Scanning Electron Micrographs of Loess and Polymer Modified Loess (a)LC, (b) HLC, (c)KH-570 LC,(d) KHLC/PAA

the characteristic absorption peak of the ester carbonyl group[21]. As depicted from Figure 2, in KHLC-PAA, the characteristic peaks near 1716 cm^{-1} and 1570 cm^{-1} were attributed to the symmetric and anti-symmetric stretching vibration absorption peak of C-O in COOH[22]. In contrast, the spectra of adsorbent retain the structure of LC except for the peaks at 1620, 1580, and 1490 cm^{-1} due to the -COO stretching vibrations of carboxylic acid, C-O stretching vibrations, and C-H stretching from CH_3, respectively. The bending vibration peak of C-H was close to 1410cm^{-1} [23]. The results showed that the co-polymers AA have been successfully grafted onto the loess surface by co-polymerization.

3.2.2. SEM Imaging Analysis

The surface morphology of the loess (LC) was observed using SEM and compared with that of its constituent materials and final product- adsorbents. The results are shown in Figure 3 (a-d). The samples were fitted and mounted on the metal holders and analyzed. Changes in the surface micro-structure of the adsorbents can be directly observed by SEM analysis. The LC surface morphology differs from that of KHLC/PAA. In LC micro-photographs, unit particles are clearly visible and the inter-particle gaps are loose. It was found that the surface of the loess particles (Figure 3(a)) was porous, uneven, and very rough, also it had many small surface cracks. After modification by HCl and KH-570 (Figure 3(b, c)), some particles were stacked on the surface, not creating too much difference. After further modification by grafting co-polymers of AA (Figure 3(d)), the surface of the loess particles became solid and compact, and a co-polymer film was formed on the loess surface, wrapping around the gaps between the particles. The SEM image of modified polymerized loess results showed that co-polymer (AA) was successfully grafted by co-polymerization onto the surface of loess particles and in the inter-particle gaps[9].

3.2.3. XRF Analysis

The XRF results show that the elemental composition of original loess remains the same after treating it with acid and silane coupling agents; there is no variation in the mineral content before and after treatment of loess clay. In the acidified loess HLC, the significant variation in the ratios of the main mineral component required for the adsorption performance of loess i.e.; SiO2 has been noticed as it has been increased after acidification. It shows that the number of silanol groups on the loess surface has been enhanced which considerably improves its absorptivity [24]. In KH-570 loess the mineral content remained similar with a little bit of variation in the composition, leading to the fact that the silane coupling agent does not alter the mineral phase composition of loess but it only enriches the already present phase composition [25].This is a representation that the loess surface has been modified and prepared for polymerization without change in overall mineral content.

Table 2. XRF Analysis Report of LC, HLC, and KHLC XRF Inspection Report. XRF-JC-2023042z

Sample (w(M)/ 10^{-2})	SiO_2	TiO_2	Al_2O_3	Fe_2O_3	MnO	MgO	CaO	Na_2O
Original Loess (LC)	61.55	0.63	11.75	4.23	0.08	2.47	6.78	1.78
Acidified Loess (HLC)	77.3	0.71	11.58	0.77	0.02	0.77	0.99	2.14
KH-570 Loess (KHLC)	34.46	2.92	50.91	1.95	0.03	0.64	2.84	0.04

3.2.4. XRD Analysis

XRD analysis was done for loess along with all three adsorbent samples to analyze chemical constituents and surface functional groups of the original loess and were compared the results with the adsorbent after the addition of the respective monomer (AA). The image obtained is given below in Figure 4.

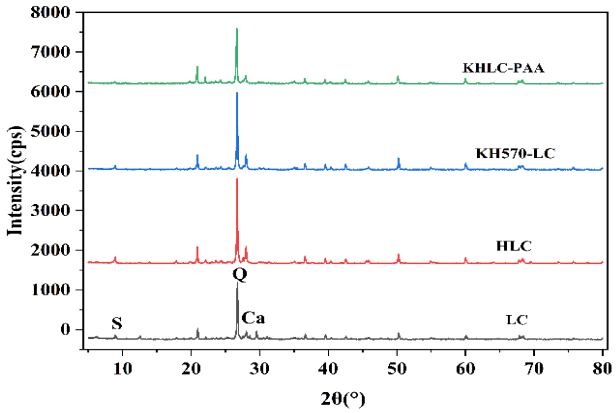

Fig. 4. X-ray diffraction patterns of LC, HLC, KH57-LC and KHLC/PAA [S – smectite, Q – quartz, Ca – calcite]

X-ray diffraction patterns of loess (LC), LC intermediates and polymerized LC(KHLC/PAA, KHLC/PAM, KHLC/PAA-AM) is shown in Figure 4. Based on the distinctive bands on the XRD spectra, the XRD data for LC shows that quartz is the primary clay mineral of loess, while calcite and smectite are the secondary minerals, depicted through MDI jade 6.0 software analysis. According to the XRD data of HLC and KHLC, the main peaks of quartz, calcite, and smectite remain similar and even are reinforced after HCl addition followed by KH570 to the loess. It depicts that the structure of loess stays intact after adding the precursor materials before polymerization. According to the figure, after the polymerization of acrylic acid onto LC in KHLC/PAA, no new peaks were noticed, which indicates that no formation of any new phase occurred. XRD data of polymerized loess depicts that the peak of diffraction for smectite is almost disappeared and the diffraction peak of calcite becomes narrow and small, which may be the result of the modification of LC by AA and AM, which have greater inter-lamellar spaces[19]. Therefore, XRD studies have indicated that after in-situ polymerization, the original crystallinity is restored and there is a significant reduction in the overall crystallinity of the final product.

3.2.4. BET Analysis of Adsorbent

The surface area and pore size distribution of LC, HLC, and KHLC/PAA had been calculated through Nitrogen adsorption-desorption isotherms as shown in Figure 2.15 and the parameters for BET isotherm are given in Table 2.5. The shape of isotherms appears to be a combination of type-II and type-IV isotherms, according to IUPAC classification. The type-II isotherm indicates the phenomenon of unrestricted monolayer-multilayer adsorption, while the type-IV isotherms characterize its hysteresis loop[26]. This can also be attributed to the condensation occurring inside mesopores, and the limiting uptake over a range of high relative pressure (p/p_o) . and the drop in the vertical axis is caused by a reduction in N_2 adsorbed at decreasing pressure values. The distribution was pore size was calculated by using the BJH (Barrett-Joyner-Halenda) method and was found to be within the mesoporous range. The surface area of LC and HLC Fig.2.15(b) is much higher showing that both the acidification has exposed the surface area of loess and they can be further polymerized well. The pore size of the materials lies between 100-200 nm with KHLC/PAA is having the highest porosity.

3.2.5. Adsorption Experiments

Overall, KHLC/PAA has shown the adsorption capacity value of 46.2mg/g with the removal efficiency of 94 % for Pb^{2+} ions; the highest removal efficiency of this adsorbent can be due to the fact that it has many active hydroxyl groups (–OH) and carboxyl group (–COOH) or carboxylates ($–COO^-$). The Pb^{2+} adsorption of by KHLC/PAA under varying parameters have been explained briefly in the following section.

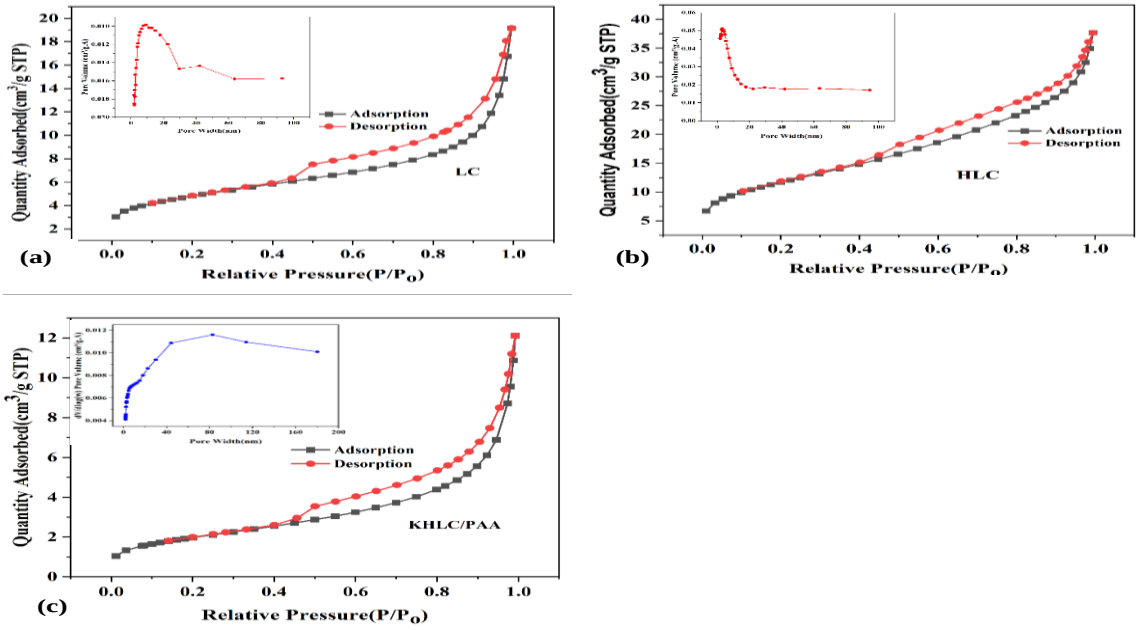

Fig. 5. BET Analysis of LC,HLC,KHLC and KHLC/PAA(a), and TG and DTG of KHLC/PAA (b)

3.2.5.1. Effect of pH value

The effect of pH on the adsorption of Pb^{2+} ions by KHLC/PAA was studied from pH range 2-9 by utilizing 0.1M NaOH and 0.1M HNO_3 with constant initial concentration (50mg.L^{-1}), at 25°C with 0.05g KHLC/PAA dosage while keeping the solution at shaker for 60 minutes. The results have been presented in Figure 6. The removal rate increases with increasing pH, as the removal percentage increases sharply from 40 to 90% at pH range 2 to 5. Reasonably, at lower pH values, the adsorbent surface was surrounded by H^+ ions, preventing metal ions from approaching the adsorption sites of the adsorbent and H^+ compete with Pb^{2+} ions for these adsorption sites, and therefore the adsorption rate decreased. With increasing pH, the number and competitive adsorption of H^+ ions decreases and therefore the surface of adsorbent becomes more negative in charge, that is why removal efficiency increases. The decrease in adsorption rate for Pb^{2+} at pH values higher than 5, can be assigned to the metal precipitation when Pb^{2+} ions begin to form precipitates in the form of lead hydroxide ($Pb(OH)_2$)), and these precipitates on the surface of KHLC/PAA prevented Pb^{2+} from interacting with the active sites. It also can cause deterioration of adsorbent surface by metal accumulation and the removal rate decreases[27].

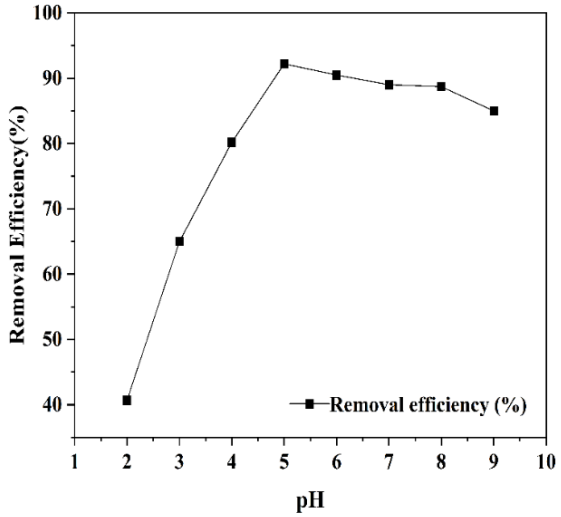

Fig. 6. Effect of pH on the adsorption of Pb^{2+} ions (Initial Concentration of Pb^{2+} ions = 50mg.L^{-1}, agitation speed = 150 rpm, Adsorbent Dosage = 0.05g, Temperature= 25°C and contact time = 60 min)

3.2.5.2. Effect of Pb^{2+} Initial Concentration

The impact of starting Pb^{2+}concentrations ranging from 20 mg.L^{-1} to 300 mg.L^{-1}, was examined at 25°C with 0.05 g of KHLC/PAA as the adsorbent, a 60-minute contact period, and a pH of 5. Figure 7 displays the adsorption capability of KHLC/PAA at different Pb^{2+} starting concentrations. As the concentration rises from 20 mg·L-1 to 50 mg·L^{-1}, the clearance efficiency quickly increases from 89% to 95%. It is possible to attribute the early stage of the adsorption process's high adsorption rate to the presence of enough active sites. When the concentration of Pb^{2+} ions was less than 100 mg-L^{-1}, the removal rate was more than 95% and decreased in a small range. When the initial concentration of Pb^{2+} ions was 50 mg-L^{-1} and the amount of Pb^{2+} ions adsorbed at equilibrium was 45.98 mg/g, the removal rate of KHLC/PAA was 95.20%. Afterwards, the removal rate decreased rapidly with increasing concentration, as only 20% removal efficiency was obtained at 300mg.L^{-1} of Pb^{2+} ions. This may be because KHLC/PAA had enough active sites to bind with Pb^{2+} ions at lower Pb^{2+} ion concentrations, and with rising Pb^{2+} concentration the availability of active sites of KHLC/PAA decreased[28]. The initial concentration can also reduce the mass transfer resistances between the aqueous phase and solid phases and it accelerates the adsorption capacity at the initial stages, during this experiment.

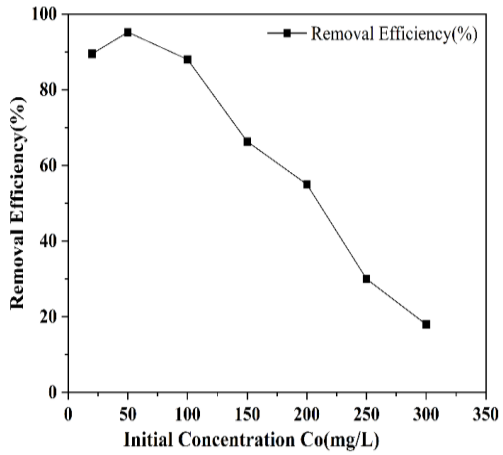

Fig. 7. Effect of Initial concentration (Pb^{2+}) on the adsorption of Pb^{2+} ions (Adsorbent dosage= 0.05g, agitation speed = 150 rpm, temperature = 25 ◦C, pH=5 and contact time = 60 min).

3.2.5.3. Effect of KHLC/PAA dosage

The adsorption studies of Pb^{2+}ions on KHLC/PAA were done by varying the quantity of adsorbent dosage from 0.02 to 0.2 g/50 mL while keeping the value of the lead solutions constant (50 mg·L^{-1}) at pH 5 for 60 minutes. Figure 8 shows that with an increase in the adsorbent dosage, the adsorption of Pb^{2+}ions also increased

noticeably. The adsorption of Pb^{2+} ions by KHLC/PAA increased abruptly from 67 to 91.4% by increasing the adsorbent dosage from 0.02 to 0.05g/50mL. The increase in removal efficiency is due to an increase in active sites on the adsorbent and greater surface area[29]. When KHLC/PAA dosage increased from 0.05 to 0.1 g, the removal rate increased slightly, and the reason is that all the active sites on the adsorbent surface are occupied with an increasing coverage, and Pb^{2+} ions must compete for the adsorption sites. An increase in the adsorbent dosage will therefore not provide higher uptake of Pb^{2+} ions[30]. After this, a slight decrease of adsorption for Pb^{2+} ions was observed from 0.1 to 0.2g/50ml, and the decrease thereof may be due to the particle interactions, such as aggregation, caused by high adsorbent concentration which in turn causes overlapping of adsorption sites as a result of over-crowding of adsorbent particles[31].

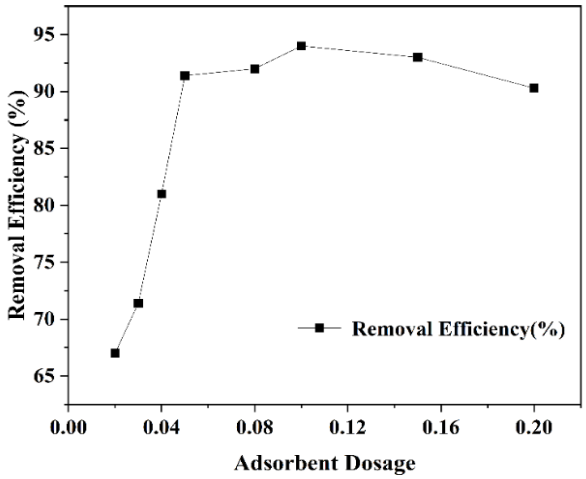

Fig. 8. Effect of Adsorbent Dosage (KHLC/PAA) on the adsorption of Pb^{2+} ions (Initial Concentration of Pb^{2+} ions = 50mg.L^{-1}, agitation speed = 150 rpm, temperature = 25 ◦C, pH=5 and contact time = 60 min)

3.2.5.4. Effect of contact time

The effect of adsorption time on Pb^{2+} ions removal was investigated at 50mL Pb^{2+} solution (50 mg·L^{-1}) at room temperature (25°C) using 0.1 g of the adsorbent KHLC/PAA, and pH 5. Time ranges of minutes and hours were applied to precisely check the variation in the adsorption phenomenon and Figure 9(a, b) shows the results. At start, the adsorption rate of Pb^{2+} ions on KHLC/PAA was relatively bit slow, moving up to 63% within 30 min. The reason behind this were two time taking processes occurring simultaneously; the Pb^{2+} in the solution initially formed a complex with the characteristic functional groups (carboxylic groups) on the adsorbent surface of KHLC/PAA, and the repulsive forces of Pb^{2+} will increase following an increase in the adsorption capacity[32]. It is also visible through the data of time in hours that no abrupt or sharp increase in rate has been observed after 60 minutes, and the removal rate remained between 95 to 96% during 24h (1440 minutes). This may be due to fact that KHLC/PAA adsorption was mainly happening on the outer surface of the material composite, which can be completed in a reasonably short time. The resistance of free Pb^{2+} ions to KHLC/PAA was also increased and adsorption saturation took longer to reach[33]. The adsorption amount of Pb^{2+} on KHLC/PAA reaches a higher value within a relatively short period (i.e., less than 1 hour) and then slowly increases and ultimately reaches a constant value after 24 hours, which indicates that Pb^{2+} adsorption went to gradual diffusion (chemisorption) within the time frame of 2 to 24 hours. This phenomenon was previously observed for the adsorption of Cu(II) on loess[34, 35].

3.2.5.5. Effect of temperature

The influence of temperatures in the range of 10°C to 50 °C on adsorption the of Pb^{2+} solution (50mg.L^{-1}) was observed using 0.1g of the adsorbent KHLC/PAA for contact time of 60 minutes, while keeping the pH 5; the results are depicted in Figure 10. With an increment of temperature from 10°C to 20°C, the rate of adsorption of KHLC/PAA on Pb^{2+} increases suggesting that heating is quite helpful in accelerating the adsorption. This may be due to the fact that, the higher the temperature, the more heavy metals get adsorbed and exchanged. When the temperature lies under the range of 20–30 ℃, the adsorption of Pb^{2+} ions increases a bit with an increase of about 3.1. As the temperature value reaches to 40 ℃, the adsorption rate decreases by 3%, which may be attributed to the slight denaturation of adsorbent particles at higher temperature. Overall, the removal rate of Pb^{2+} ions was more than 91% at high as well as low temperatures, and the maximum removal rate of Pb^{2+} ions was 95.5% at 30°C. The overall influence of the temperature on the adsorption process was not much promising and adsorption of Pb^{2+} ions was mostly temperature-independent[36].

.

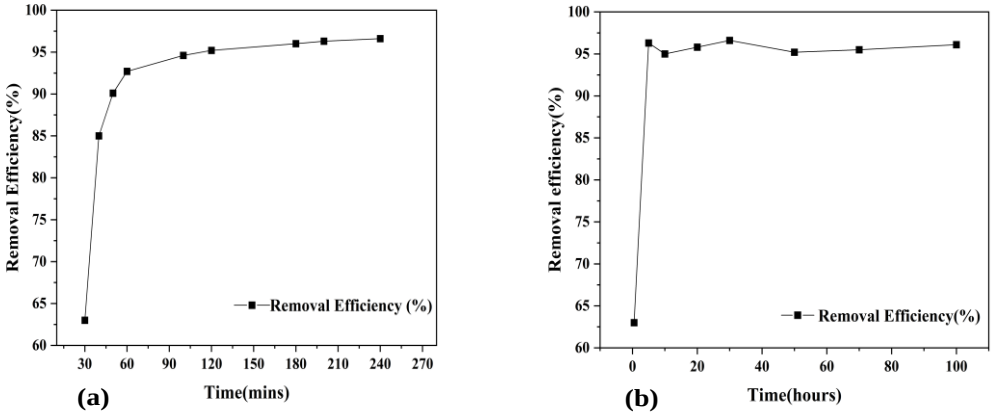

Fig. 9. Effect of contact time on the adsorption of Pb^{2+} ions;Time in Minutes (a), Time in Hours (b) (Initial Concentration of Pb^{2+} ions = 50mg.L^{-1}, agitation speed = 150 rpm, temperature = 25 ◦C, pH=5 and adsorbent dosage =0.1g).

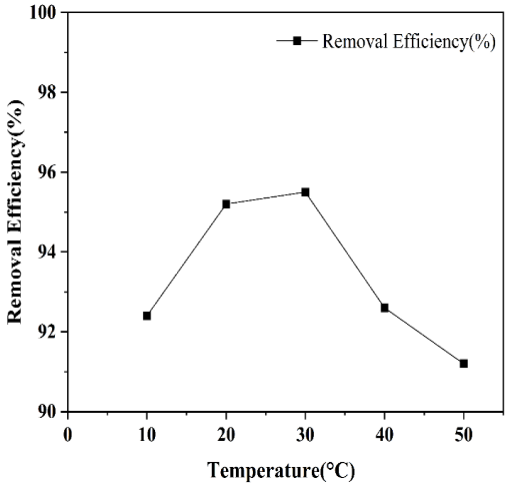

Fig. 10. Effect of Temperature on the adsorption of Pb^{2+} ions (Initial Concentration of Pb^{2+} ions = 50mg.L^{-1}, agitation speed = 150 rpm, Adsorbent Dosage = 0.1g, pH=5 and contact time = 60 min)

3.3. Adsorption Isotherms

Freundlich isothermal and Langmuir isothermal models were applied to study the adsorption isotherms for Pb^{2+} ions by KHLC/PAA, and the relationship between concentration and adsorption capacity was evaluated by non-linear fitting. The isothermal adsorption equations of KHLC/PAA for Pb^{2+} adsorption is calculated as per equations 3 and 4, representing the Langmuir and Freundlich isothermal equations, respectively. The Langmuir isotherm equation is given as follows[9, 37]

$$\frac{C_e}{q_e} = \frac{C_e}{q_m} + \frac{1}{q_m . K_L} \qquad \text{Equation 3}$$

Here q_e represents the amount of pollutant adsorbed at equilibrium stage (mg/g), while C_e points towards the equilibrium concentration (mg/L). q_m is the Langmuir constants indicating the adsorption capacity (maximum) and K_L is the other Langmuir constant which shows energy of adsorption, also called binding constant. The Langmuir adsorption model postulated that the adsorbate would cover the adsorbent surface in a monolayer. Adsorption is assumed to occur at certain homogeneous sites inside the adsorbent, and the model also assumes uniform energy of adsorption onto the surface. According to the experimental the Langmuir adsorption model fits in the experiment. Langmuir isotherm was well fitted into this plot of qe versus Ce developed as straight-line plot between both the variables, (Figure 11(a)); the value of q_m and the K_L were determined from the measured slope and intercepts of the qe versus Ce, given in Table 3. The maximum adsorption capacity obtained was 159 mg·g^{-1} and the value regression co-efficient (R^2) was 0.991, both suggesting the best fitting of Pb^{2+} adsorption data onto KHLC/PAA into Langmuir equation and the Langmuir isothermal model.

The Freundlich isotherm gives an empirical equation and it can be expressed by the following equation[37]

$$\ln q_e = n \ln C_e + \ln K_F \qquad \text{Equation 4}$$

K_F and n are referred to Freundlich constants, where the K_F indicates the capacity of the adsorbent and n refers to the favorability. Freundlich adsorption isotherm was also fitted into the plot between C_e and q_e and values of K_F and n were calculated from the slopes and intercepts values of the plot between C_e versus q_e (Figure 11(b)) are shown in Table 3. The coefficient of correlation is 0.97 (<0.99) with n value < 1, indicating that the Langmuir isotherm is much more favorable and suitable to describe the processes of adsorption of Pb^{2+} onto KHLC/PAA than the Freundlich isotherm. The saturated adsorption amounts of Pb^{2+} by 0.1

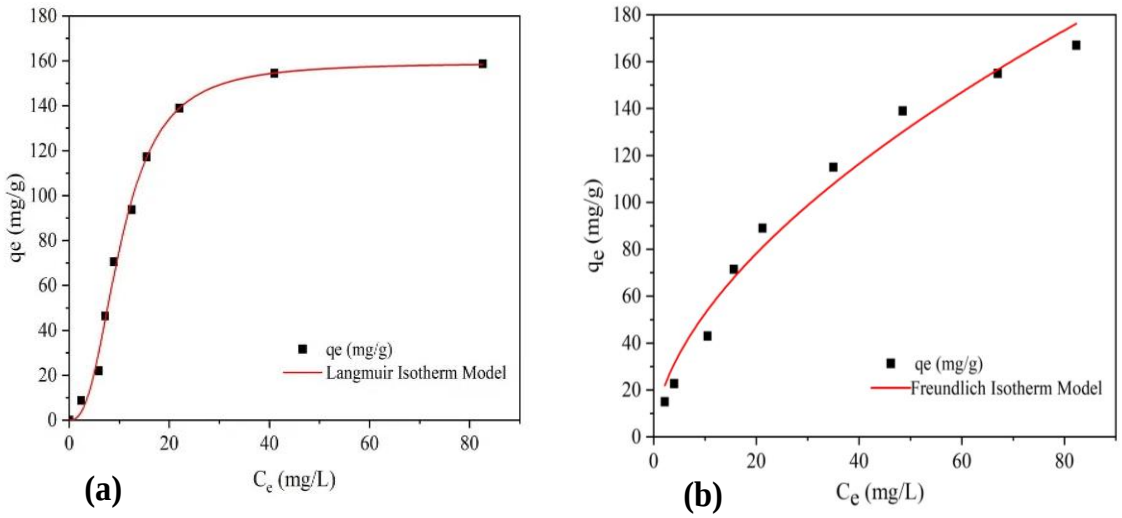

Fig. 11. Isotherms model of Pb^{2+} onto KHLC/PAA, Langmuir (a) and Freundlich (b)

Table 3. Parameters of Langmuir and Freundlich Isotherms

Langmuir			Freundlich		
$q_m(mg.g^{-1})$	K_L	R^2	1/n	K_F	R^2
159.11	0.0024	0.99	13.9	0.57	0.97

3.4. Adsorption Kinetics

Additionally, pseudo first order and pseudo second order kinetic models were used to study the adsorption process. Equations 5 and 6 the pseudo first and pseudo second order model equations, respectively, were applied to the experimental data to compute it using adsorption kinetics. The pseudo first order kinetic model states that the number of occupied sites is directly proportional to the number of unoccupied sites. In contrast, the pseudo second order kinetic model assumes a chemical reaction mechanism of the adsorption process and it also proposes that rate of adsorption is controlled through chemical adsorption by the sharing or exchange of electrons between the adsorbent and adsorbate. pseudo first order kinetic model states that the number of occupied sites is directly proportional to the number of unoccupied sites. The parameters of adsorption kinetics are calculated by the following equations 5 and 6[38].

$$(q_e - q_t) = -K^1 t + \ln. q_e \qquad \text{Equation 5}$$

$$\frac{t}{q_t} = \frac{t}{q_e} + \frac{1}{K_2 . q_e^2} \qquad \text{Equation 6}$$

Here q_e indicates the Pb^{2+} ions adsorption amount per unit mass of adsorbent ($mg.g^{-1}$) at the equilibrium point, q_t indicates the amount of Pb^{2+} adsorbed ($mg.g^{-1}$) at the particular time t (min), $k_1$and k_2 are the adsorption rate constants for the first order reaction and the second order reaction models, respectively. Non-linear equations were more effective than the linear equations for the measurement of parameters of kinetic models and Figure 12 and Table 4 show the calculated results. It was very clear that the pseudo second-order kinetic model established between time (t) and t/qt (Figure 12(b)) was very suitable in describing the adsorption kinetics. In the parameters of pseudo-second order, the calculated value of q_e (cal(mg/g))= 48 is very close to the experimental value of q_e (q_e(exp(mg/g)), and the higher determination coefficient value R^2 was found to be 0.998, in contrast to the pseudo-first-order model established between t and q_t (Figure 12(a)) , which shows lesser value of correlation coefficient (R^2 = 0.80) with lower value of q_e(cal) than q_e(exp(mg/g)), also chemical adsorption has done a significant role in the adsorption process and the determination coefficient (R^2 = 0.998) indicates that chemical reaction is mainly the rate-controlling step[32]. The values of rate constants k_1,k_2 along with q_e (cal(mg/g)) and those of correlation coefficient R^2 are summed up in Table 4. The conditions were kept as 50 mg/L of Pb^{2+} solution at temperature 25~30 °C and pH 5.0

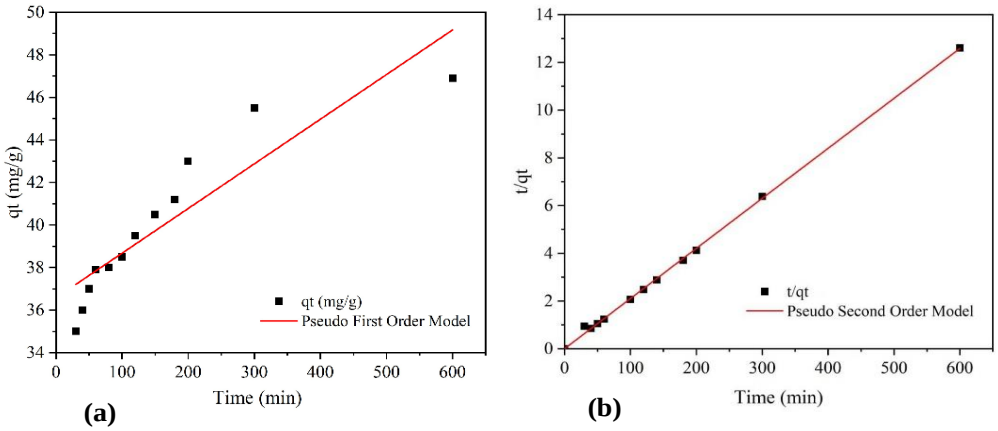

Fig. 12. Kinetic models of Pb^{2+} onto KHLC/PAA. Pseudo first-order and (a), Pseudo second order (b)

Table 4. Parameters of Pseudo first-order and Pseudo second-order kinetic models C_e (mg/L) = 50, q_e(exp.) (mg/g) = 48.3

Pseudo-first-order kinetics			Pseudo-second-order kinetics		
q_e(mg.g^{-1})	K_1(min^{-1})	R^2	q_e(mg.g^{-1})	K_2(g/mg.min^{-1})	R^2
47.3	1.19*10^{-3}	0.80	48	1.18*10^{-5}	0.99

3.5. Adsorption Thermodynamics

Using the statistical physical model, thermodynamic functions for the ternary adsorption of tested adsorbates and modified adsorbents can be computed. Thermodynamic parameters i.e., Gibbs free energy, Entropy, and internal energy were calculated in this section. The thermodynamic standard equations were used to evaluate the thermodynamic behavior for the adsorption of Pb^{2+} ions on KHLC/PAA. Thermodynamic equations 7 and 8, are given following[39].

$$\Delta G_o = -RT.\ln K_c \quad \text{Equation 7}$$

$$\Delta G_o = \Delta H_o - T.\Delta S \quad \text{Equation 8}$$

Where K_c means the distribution coefficient of solute between the solution and the adsorbent at equilibrium (q_e/C_e), R represents ideal gas constant (R=8.314), T indicated temperature (K), ΔH_o is the enthalpy change, ΔS_o is the entropy change and ΔG_o indicates the change in Gibbs' free energy.

The slope and intercept of the developed linearized curve were utilized to determine enthalpy change (ΔH_o) and the change of entropy (ΔS_o) as demonstrated in Figure 13 fitting with Equation 8. The concentration of solute and temperature change greatly influence the thermodynamic parameters as depicted in from Table 5. At a fixed initial concentration of solute, the calculated values of Gibbs' free energy shows decreasing trend with the increasing reaction temperature, which means that Pb^{2+} adsorption is not dependent on temperature. Furthermore, the Gibbs' free energy change was negative indicating that this was spontaneous adsorption process in the temperature range of 283K to 323K. The change of free energy(ΔG_o) was spontaneous as well as feasible at all given temperatures. The calculated values enthalpy change (ΔH_o) were negative pointing towards an endothermic character to the overall adsorption process and ΔS_o values shows increasing disorder value in the system; therefore, the nature of the reaction between Pb^{2+} and KHLC/PAA was endothermic.

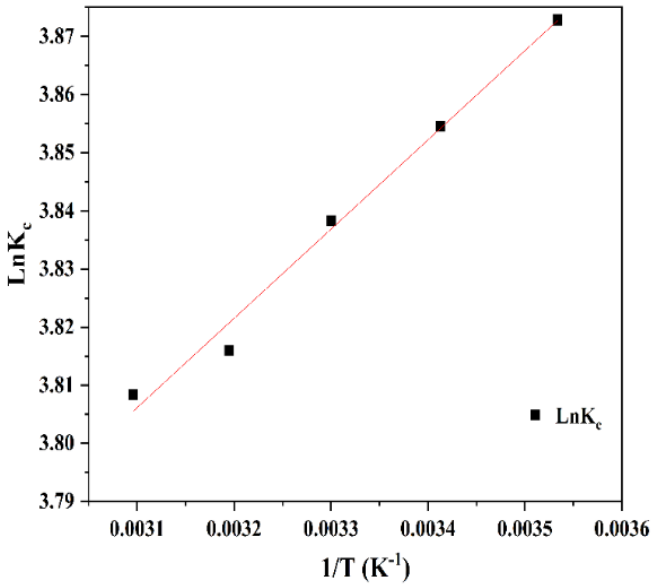

Fig. 13. Linear fit of thermodynamics for Pb^{2+} adsorption on KHLC/PAA.

Table 5. Thermodynamic Parameters for Pb^{2+} adsorption on KHLC/PAA

T(K)	ΔG_o(kJmol^{-1})	ΔH_o(kJmol^{-1})	ΔS(Jmol^{-1} K^{-1})
273	-9111.96		
293	-9388.85	-1276.03	27.68
298	-9527.29		
313	-9942.62		
323	-10219.5		

3.6. Re-usability of KHLC/PAA for Pb^{2+}ions

Good re-usability indicates much about the development prospect of the adsorbent and it makes adsorption process more beneficial economically. To evaluate this aspect, five cycles of adsorption-desorption experiments for Pb^{2+} ions by KHLC/PAA were conducted, and the results are shown in Figure 14. The equation 1 was implemented to evaluate adsorption cycle efficiency. There was reduction in adsorption capacity of KHLC/PAA with an increase in the number of adsorption cycles; the first cycle starts with 85% adsorption rate for Pb^{2+} ions and then goes on declining gradually. Some contaminants are not completely separated from the adsorbent, and it is normal for the adsorption capacity to decrease slightly with each cycle. However, after the 5th cycle, there was a significant drop in the adsorption capacity of KHLC/PAA, when the adsorption capacity decreased by about 10% from 76% in 4th cycle to 66% in 5th cycle for Pb^{2+}. In the light of the results depicted in Figure 14, it is concluded that the adsorbent has good and satisfactory adsorption performance and re-usability, and it can be recovered and reused easily.

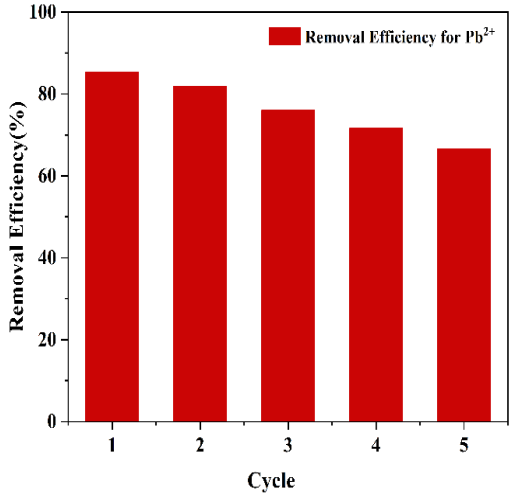

Fig. 14. Reusability/Recycling of KHLC/PAA for Pb^{2+} adsorption

3.7. Adsorption Mechanism

The adsorption mechanism of KHLC/PAA was discussed by the investigation of vibration absorption peaks using FTIR spectra. Figure 15 depicts the comparison of FTIR spectra of KHLC/PAA and KHLC/PAA loaded with Pb^{2+} ions (KHLC/PAA-Pb). The band of absorption at 1703cm^{-1} expanded in KHLC/PAA after adsorption, simultaneously, the weak smaller bands at 1401cm^{-1} and 1284cm^{-1} were disappeared and the band at 1035 cm^{-1} was shrunken in KHLC/PAA-Pb^{2+}. These bands represent the C-O group, and it has shown that C-O and COO^- were the actual and active sites of adsorption for Pb^{2+} ions on KHLC/PAA. The peak at 3625cm^{-1} shows a stretching vibration peak of the -OH group. In other words, complexation had been developed between carboxyl group of KHLC/PAA and Pb^{2+} and -OH groups when deprotonated, also contributed to adsorption through electrostatic interactions. Rapid (almost in an hour) and reversible adsorption of Pb^{2+} ions supports the involvement of outer sphere complexation/cation exchange mechanism for the heavy metals' removal. Therefore, the elimination of Pb^{2+} ions is also contributed by cation exchange between pb^{2+} metal ions and the other inorganic metal ions i.e.; Mn^{2+}, $Ca^{2+}$and Mg^{2+} attached to loess.

The following equations 9 and 10 explain the possible mechanism of Pb^{2+} ions adsorption by KHLC/PAA.

$$2\,(-COOH) + Me^{2+} \rightarrow (CO_2)_2 + 2H \quad \text{Equation 9}$$

$$-COOH + Me^{2+} \rightarrow -CO_2Me + H^+ \quad \text{Equation 10}$$

Where -COOH represents the main functional group (carboxyl) of the KHLC/PAA and Me^{2+} represents lead (II) metal.

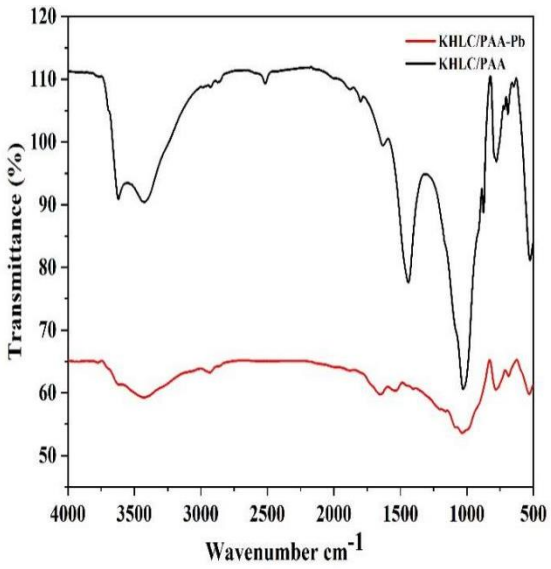

Fig. 15. FTIR spectra of KHLC/PAA and KHLC/PAA-Pb^{2+}

3.8. Conclusion

KHLC/PAA was most effective adsorbent for the removal of Pb^{2+} ions from wastewater and it has depicted an adsorption capacity of about 46mg/g. The overall adsorption of Pb^{2+} ions on KHLC/PAA is influenced by initial metal ion concentration, solution pH, contact time, adsorbent dosage, and reaction temperature. Adsorption kinetics were relatively fast i.e.; reaching equilibrium in about 1 hour, and the non-linearized fitting of the pseudo-second-order model well elaborated the data. The Pb(II) adsorption on KHLC/PAA was well fitted to the Langmuir mono-layer adsorption model, showing the isothermal equation of the Langmuir model to be much more suitable for the evaluation of test data. The thermodynamic data also proved the adsorption of Pb^{2+} on KHLC/PAA to be spontaneous, feasible, and endothermic. At 25°C and pH 5, the calculated maximum adsorption capacity (q_m) for Pb^{2+} ions on KHLC/PAA was 159.1mg/g, with the maximum removal efficiency was 92.2%. The mechanism of adsorption was evaluated to be surface complexation and ion exchange, according to the FTIR data of KHLC/PAA-Pb. The adsorbent could be easily regenerated by using 0.1mol/L HCl solution, and the adsorbent depicted a reasonable re-usability after five cycles. In conclusion, loess-based polymerized adsorbent "KHLC/PAA" can be an important and inexpensive adsorbent for the removal of heavy metal Pb^{2+} ions from polluted water.

References

[1] K. Sharma, S. Rajan, S. Nayak, Water pollution: Primary sources and associated human health hazards with special emphasis on rural areas, 2023.

[2] N. Zhang, N. Cheng, Q. Liu, Functionalized Biomass Carbon-Based Adsorbent for Simultaneous Removal of Pb(2+) and MB in Wastewater, Materials (Basel) 14 (2021).

[3] J. Wang, R. Chen, L. Fan, L. Cui, Y. Zhang, J. Cheng, X. Wu, W. Zeng, Q. Tian, L. Shen, Construction of fungi-microalgae symbiotic system and adsorption study of heavy metal ions, Separation and Purification Technology 268 (2021) 118689.

[4] Y. Zhou, X. Liu, Y. Xiang, P. Wang, J. Zhang, F. Zhang, J. Wei, L. Luo, M. Lei, L. Tang, Modification of biochar derived from sawdust and its application in removal of tetracycline and copper from aqueous solution: Adsorption mechanism and modelling, Bioresource Technology 245 (2017) 266-273.

[5] Y. Zhang, Z. Li, Heavy metals removal using hydrogel-supported nanosized hydrous ferric oxide: Synthesis, characterization, and mechanism, Sci Total Environ 580 (2017) 776-786.

[6] C. Gao, X. Zhang, Y. Yuan, Y. Lei, J. Gao, S. Zhao, C. He, L. Deng, Removal of hexavalent chromium ions by core-shell sand/Mg-layer double hydroxides (LDHs) in constructed rapid infiltration system, Ecotoxicology and Environmental Safety 166 (2018) 285-293.

[7] W. Huang, J. Xu, D. Lu, J. Deng, G. Shi, T. Zhou, Rational design of magnetic infinite coordination polymer core-shell nanoparticles as recyclable adsorbents for selective removal of anionic dyes from colored wastewater, Applied Surface Science 462 (2018) 453-465.

[8] M. Rafatullah, O. Sulaiman, R. Hashim, A. Ahmad, Adsorption of copper (II), chromium (III), nickel (II) and lead (II) ions from aqueous solutions by meranti sawdust, Journal of Hazardous Materials 170 (2009) 969-977.

[9] Yue, Z., et al., Removal of chromium Cr(VI) by low-cost chemically activated carbon materials from water. Journal of hazardous materials, 2009. **166 1**: p. 74-8.

[10] F. Tang, D. Gao, L. Wang, Y. He, P. Song, R. Wang, Preparation of grafting copolymer of acrylic acid onto loess surface and its adsorption behavior, Water Science and Technology 82 (2020) 673-682.

[11] S. Chakravarty, A. Mohanty, T.N. Sudha, A.K. Upadhyay, J. Konar, J.K. Sircar, A. Madhukar, K.K. Gupta, Removal of Pb(II) ions from aqueous solution by adsorption using bael leaves (Aegle marmelos), J Hazard Mater 173 (2010) 502-509.

[12 M. Ahmaruzzaman, V.K. Gupta, Rice Husk and Its Ash as Low-Cost Adsorbents in Water and Wastewater Treatment, Industrial & Engineering Chemistry Research 50 (2011) 13589-13613.

[13] Z. Yue, S.E. Bender, J. Wang, J. Economy, Removal of chromium Cr(VI) by low-cost chemically activated carbon

materials from water, Journal of hazardous materials 166 1 (2009) 74-78.
[14] K.A. Mumford, K.A. Northcott, D.C. Shallcross, I. Snape, G.W. Stevens, Comparison of Amberlite IRC-748 Resin and Zeolite for Copper and Ammonium Ion Exchange, Journal of Chemical & Engineering Data 53 (2008) 2012-2017.
[15] M.-q. Jiang, X.-y. Jin, X.-Q. Lu, Z.-l. Chen, Adsorption of Pb(II), Cd(II), Ni(II) and Cu(II) onto natural kaolinite clay, Desalination 252 (2010) 33-39.
[16] A. Battaglia, N. Calace, E. Nardi, B.M. Petronio, M. Pietroletti, Paper mill sludge–soil mixture: kinetic and thermodynamic tests of cadmium and lead sorption capability, Microchemical Journal 75 (2003) 97-102.
[17] Y. Wang, X. Tang, Y. Chen, L. Zhan, Z. Li, Q. Tang, Adsorption behavior and mechanism of Cd(II) on loess soil from China, Journal of Hazardous Materials 172 (2009) 30-37.
[18] X. Tang, Z. Li, Y. Chen, Adsorption behavior of Zn(II) on calcinated Chinese loess, Journal of Hazardous Materials 161 (2009) 824-834.
[19] S. Xing, M. Zhao, Z. Ma, Removal of heavy metal ions from aqueous solution using red loess as an adsorbent, Journal of Environmental Sciences 23 (2011) 1497-1502.
[20] Y.-F. He, L. Zhang, R.-M. Wang, H.-R. Li, Y. Wang, Loess clay based copolymer for removing Pb(II) ions, Journal of Hazardous Materials 227-228 (2012) 334-340.
[21] A. Jahanbakhsh, S. Pirsa, M. Bahram, Synthesis and characterization of magnetic nanocomposites based on Hydrogel-Fe 3O 4 and application to remove of organic dye from waste water. Main Group Chemistry 16(2017) 85-94.
[22] S. Mostafavi, V. Rezaverdinejad, S. Pirsa, Design and fabrication of nanocomposite-based polyurethane filter for improving municipal waste water quality and removing organic pollutants. Adsorption Science & Technology, 37(2019):95-112.
[23] F. Asadzadeh, S. Pirsa,. Specific removal of nitrite from Lake Urmia sediments by biohydrogel based on isolated soy protein/tragacanth/mesoporous silica nanoparticles/lycopene. Global Challenges. 2020 (2020) 2000061.
[24] F. Asadzadeh, S. Pirsa, Zein/EDTA/chlorophyll/nano-clay biocomposite sorbent: Investigation physicochemical properties sorbent and its ability to remove contaminants of industrial wastewater. Journal of Polymers and the Environment. 30 (2022):2109-27.
[25] S. Pirsa, M. Alizadeh M, N. Ghahremannejad,. Application of nano-sized poly N-phenyl pyrrole coated polyester fiber to headspace microextraction of some volatile organic compounds and analysis by gas chromatography. Current Analytical Chemistry. 12(2016):457-64.
[26] A. Saidfar, M. Alizadeh, S. Pirsa,. Application of nano-sized poly (N-methyl pyrrole-pyrrole) fiber to the headspace solid-phase microextraction of volatile organic compounds from yogurt. Journal of Chemistry Letters. 1(2020) 39-46.
[27] S. Kalantari, L. Roufegarinejad, S. Pirsa, M. Gharekhani, Green extraction of bioactive compounds of pomegranate peel using β-Cyclodextrin and ultrasound. Main Group Chemistry, 1 (2020):61-80.
[28] S. Pirsa, F. Asadzadeh. Synthesis of Fe3O4/SiO2/Polypyrrole magnetic nanocomposite polymer powder: Investigation of structural properties and ability to purify of edible sea salts. Advanced Powder Technology. 32(2021):1233-46.
[29] C.L. Narayana Reddy, B.Y. Swamy, C.V. Prasad, K. Madhusudhan Rao, M.N. Prabhakar, C. Aswini, M.C.S. Subha, K.C. Rao, Development and Characterization of Chitosan-Poly (Vinyl Pyrrolidone) Blend Microspheres for Controlled Release of Metformin Hydrochloride, International Journal of Polymeric Materials and Polymeric Biomaterials 61 (2012) 424-436.
[30] X. Liu, X. Bai, L. Dong, J. Liang, Y. Jin, Y. Wei, Y. Li, S. Huang, J. Qu, Composting enhances the removal of lead ions in aqueous solution by spent mushroom substrate: Biosorption and precipitation, Journal of Cleaner Production 200 (2018) 1-11.
[31] S. Jin, J. Gu, Y. Shi, K. Shao, X. Yu, G. Yue, Preparation and electrical sensitive behavior of poly (N-vinylpyrrolidone-co-acrylic acid) hydrogel with flexible chain nature, European Polymer Journal 49 (2013) 1871-1880.
[32] E. Rafiee, M. Joshaghani, P.G.-S. Abadi, Effect of a weak magnetic field on the Mizoroki–Heck coupling reaction in the presence of wicker-like palladium-poly(N-vinylpyrrolidone)-iron nanocatalyst, Journal of Magnetism and Magnetic Materials 408 (2016) 107-115.
[33] Y. Shen, H. Yan, R. Wang, P. Song, Y. He, Review: Progress with Functional Materials Based on Loess Particles, Clays and Clay Minerals 69 (2021) 301-314.
[34] C. Zhang, X. Wang, Z. Hu, Q. Wu, H. Zhu, J. Lu, Long-term performance of silane coupling agent/metakaolin based geopolymer, Journal of Building Engineering 36 (2021) 102091.
[35] D. Saini, S. Tripathy, A. Kumar, S. Sharma, A. Ghosh, D. Bhattacharya, Impedance and modulus spectroscopic analysis of single phase BaZrO3 ceramics for SOFC application, Ionics 24 (2018).
[36] U. Farooq, J.A. Kozinski, M.A. Khan, M. Athar, Biosorption of heavy metal ions using wheat based biosorbents – A review of the recent literature, Bioresource Technology 101 (2010) 5043-5053.
[37] D. Sun, X. Zhang, Y. Wu, X. Liu, Adsorption of anionic dyes from aqueous solution on fly ash, Journal of Hazardous Materials 181 (2010) 335-342.
[38] V.K. Garg, R. Gupta, R. Kumar, R.K. Gupta, Adsorption of chromium from aqueous solution on treated sawdust, Bioresource Technology 92 (2004) 79-81.
[39] M.K. Aroua, S.P.P. Leong, L.Y. Teo, C.Y. Yin, W.M.A.W. Daud, Real-time determination of kinetics of adsorption of

lead(II) onto palm shell-based activated carbon using ion selective electrode, Bioresource Technology 99 (2008) 5786-5792.
[1] K. Sharma, S. Rajan, S. Nayak, Water pollution: Primary sources and associated human health hazards with special emphasis on rural areas, 2023.
[2] N. Zhang, N. Cheng, Q. Liu, Functionalized Biomass Carbon-Based Adsorbent for Simultaneous Removal of Pb(2+) and MB in Wastewater, Materials (Basel) 14 (2021).
[3] J. Wang, R. Chen, L. Fan, L. Cui, Y. Zhang, J. Cheng, X. Wu, W. Zeng, Q. Tian, L. Shen, Construction of fungi-microalgae symbiotic system and adsorption study of heavy metal ions, Separation and Purification Technology 268 (2021) 118689.
[4] Y. Zhou, X. Liu, Y. Xiang, P. Wang, J. Zhang, F. Zhang, J. Wei, L. Luo, M. Lei, L. Tang, Modification of biochar derived from sawdust and its application in removal of tetracycline and copper from aqueous solution: Adsorption mechanism and modelling, Bioresource Technology 245 (2017) 266-273.
[5] Y. Zhang, Z. Li, Heavy metals removal using hydrogel-supported nanosized hydrous ferric oxide: Synthesis, characterization, and mechanism, Sci Total Environ 580 (2017) 776-786.
[6] C. Gao, X. Zhang, Y. Yuan, Y. Lei, J. Gao, S. Zhao, C. He, L. Deng, Removal of hexavalent chromium ions by core-shell sand/Mg-layer double hydroxides (LDHs) in constructed rapid infiltration system, Ecotoxicology and Environmental Safety 166 (2018) 285-293.
[7] W. Huang, J. Xu, D. Lu, J. Deng, G. Shi, T. Zhou, Rational design of magnetic infinite coordination polymer core-shell nanoparticles as recyclable adsorbents for selective removal of anionic dyes from colored wastewater, Applied Surface Science 462 (2018) 453-465.
[8] M. Rafatullah, O. Sulaiman, R. Hashim, A. Ahmad, Adsorption of copper (II), chromium (III), nickel (II) and lead (II) ions from aqueous solutions by meranti sawdust, Journal of Hazardous Materials 170 (2009) 969-977.
[9] F. Tang, D. Gao, L. Wang, Y. He, P. Song, R. Wang, Preparation of grafting copolymer of acrylic acid onto loess surface and its adsorption behavior, Water Science and Technology 82 (2020) 673-682.
[10] S. Chakravarty, A. Mohanty, T.N. Sudha, A.K. Upadhyay, J. Konar, J.K. Sircar, A. Madhukar, K.K. Gupta, Removal of Pb(II) ions from aqueous solution by adsorption using bael leaves (Aegle marmelos), J Hazard Mater 173 (2010) 502-509.
[11] M. Ahmaruzzaman, V.K. Gupta, Rice Husk and Its Ash as Low-Cost Adsorbents in Water and Wastewater Treatment, Industrial & Engineering Chemistry Research 50 (2011) 13589-13613.
[12] Z. Yue, S.E. Bender, J. Wang, J. Economy, Removal of chromium Cr(VI) by low-cost chemically activated carbon materials from water, Journal of hazardous materials 166 1 (2009) 74-78.
[13] K.A. Mumford, K.A. Northcott, D.C. Shallcross, I. Snape, G.W. Stevens, Comparison of Amberlite IRC-748 Resin and Zeolite for Copper and Ammonium Ion Exchange, Journal of Chemical & Engineering Data 53 (2008) 2012-2017.
[14] M.-q. Jiang, X.-y. Jin, X.-Q. Lu, Z.-l. Chen, Adsorption of Pb(II), Cd(II), Ni(II) and Cu(II) onto natural kaolinite clay, Desalination 252 (2010) 33-39.
[15] A. Battaglia, N. Calace, E. Nardi, B.M. Petronio, M. Pietroletti, Paper mill sludge–soil mixture: kinetic and thermodynamic tests of cadmium and lead sorption capability, Microchemical Journal 75 (2003) 97-102.
[16] Y. Wang, X. Tang, Y. Chen, L. Zhan, Z. Li, Q. Tang, Adsorption behavior and mechanism of Cd(II) on loess soil from China, Journal of Hazardous Materials 172 (2009) 30-37.
[17] X. Tang, Z. Li, Y. Chen, Adsorption behavior of Zn(II) on calcinated Chinese loess, Journal of Hazardous Materials 161 (2009) 824-834.
[18] S. Xing, M. Zhao, Z. Ma, Removal of heavy metal ions from aqueous solution using red loess as an adsorbent, Journal of Environmental Sciences 23 (2011) 1497-1502.
[19] Y.-F. He, L. Zhang, R.-M. Wang, H.-R. Li, Y. Wang, Loess clay based copolymer for removing Pb(II) ions, Journal of Hazardous Materials 227-228 (2012) 334-340.
[20] C.L. Narayana Reddy, B.Y. Swamy, C.V. Prasad, K. Madhusudhan Rao, M.N. Prabhakar, C. Aswini, M.C.S. Subha, K.C. Rao, Development and Characterization of Chitosan-Poly (Vinyl Pyrrolidone) Blend Microspheres for Controlled Release of Metformin Hydrochloride, International Journal of Polymeric Materials and Polymeric Biomaterials 61 (2012) 424-436.
[21] X. Liu, X. Bai, L. Dong, J. Liang, Y. Jin, Y. Wei, Y. Li, S. Huang, J. Qu, Composting enhances the removal of lead ions in aqueous solution by spent mushroom substrate: Biosorption and precipitation, Journal of Cleaner Production 200 (2018) 1-11.
[22] S. Jin, J. Gu, Y. Shi, K. Shao, X. Yu, G. Yue, Preparation and electrical sensitive behavior of poly (N-vinylpyrrolidone-co-acrylic acid) hydrogel with flexible chain nature, European Polymer Journal 49 (2013) 1871-1880.
[23] E. Rafiee, M. Joshaghani, P.G.-S. Abadi, Effect of a weak magnetic field on the Mizoroki–Heck coupling reaction in the presence of wicker-like palladium-poly(N-vinylpyrrolidone)-iron nanocatalyst, Journal of Magnetism and Magnetic Materials 408 (2016) 107-115.
[24] Y. Shen, H. Yan, R. Wang, P. Song, Y. He, Review: Progress with Functional Materials Based on Loess Particles, Clays and Clay Minerals 69 (2021) 301-314.
[25] C. Zhang, X. Wang, Z. Hu, Q. Wu, H. Zhu, J. Lu, Long-term performance of silane coupling agent/metakaolin based geopolymer, Journal of Building Engineering 36 (2021) 102091.
[26] D. Saini, S. Tripathy, A. Kumar, S. Sharma, A. Ghosh, D. Bhattacharya, Impedance and modulus spectroscopic

analysis of single phase BaZrO3 ceramics for SOFC application, Ionics 24 (2018).
[27] U. Farooq, J.A. Kozinski, M.A. Khan, M. Athar, Biosorption of heavy metal ions using wheat based biosorbents – A review of the recent literature, Bioresource Technology 101 (2010) 5043-5053.
[28] D. Sun, X. Zhang, Y. Wu, X. Liu, Adsorption of anionic dyes from aqueous solution on fly ash, Journal of Hazardous Materials 181 (2010) 335-342.
[29] V.K. Garg, R. Gupta, R. Kumar, R.K. Gupta, Adsorption of chromium from aqueous solution on treated sawdust, Bioresource Technology 92 (2004) 79-81.
[30] M.K. Aroua, S.P.P. Leong, L.Y. Teo, C.Y. Yin, W.M.A.W. Daud, Real-time determination of kinetics of adsorption of lead(II) onto palm shell-based activated carbon using ion selective electrode, Bioresource Technology 99 (2008) 5786-5792.
[31] C. Namasivayam, D. Prabha, M. Kumutha, Removal of direct red and acid brilliant blue by adsorption on to banana pith, Bioresource Technology 64 (1998) 77-79.
[32] Y.S. Ho, G. McKay, Pseudo-second order model for sorption processes, Process Biochemistry 34 (1999) 451-465.
[33] M. Doğan, H. Abak, M. Alkan, Adsorption of methylene blue onto hazelnut shell: Kinetics, mechanism and activation parameters, Journal of Hazardous Materials 164 (2009) 172-181.
[34] X.W. Tang, Z.Z. Li, Y.M. Chen, Y. Wang, Removal of Cu(II) from aqueous solution by adsorption on Chinese Quaternary loess: Kinetics and equilibrium studies, Journal of Environmental Science and Health, Part A 43 (2008) 779-791.
[35] X.W. Tang, Z.Z. Li, Y.M. Chen, Y. Wang, Removal of Cu(II) from aqueous solution by adsorption on Chinese Quaternary loess: kinetics and equilibrium studies, J Environ Sci Health A Tox Hazard Subst Environ Eng 43 (2008) 779-791.
[36] L. Guo, C.-m. Sun, G.-y. Li, C.-p. Liu, C.-n. Ji, Thermodynamics and kinetics of Zn(II) adsorption on crosslinked starch phosphates, Journal of Hazardous Materials 161 (2009) 510-515.
[37] A.E. Ofomaja, Equilibrium sorption of methylene blue using mansonia wood sawdust as biosorbent, Desalination and Water Treatment 3 (2009) 1-10.
[38] Z. Raji, A. Karim, A. Karam, S. Khalloufi, Adsorption of Heavy Metals: Mechanisms, Kinetics, and Applications of Various Adsorbents in Wastewater Remediation—A Review, Waste 1 (2023) 775-805.
[39] T.A. Saleh, Chapter 3 - Kinetic models and thermodynamics of adsorption processes: classification, in: T.A. Saleh (Ed.), Interface Science and Technology, Elsevier2022, pp. 65-97.